ROCKFALL MODELLING: METHODS AND MODEL APPLICATION IN AN ALPINE BASIN (REINTAL, GERMANY)

Volker Wichmann & Michael Becht

Lehrstuhl für Physische Geographie – Katholische Universität Eichstätt-Ingolstadt – Ostenstr. 18 – 85072 Eichstätt

Abstract: Computer simulation models allow to assess the risk posed by rockfall in an efficient way. In this paper we give a review of several rockfall models we implemented as SAGA module libraries. In all cases, rockfall source areas are identified by applying a threshold to a slope gradient map. Starting from these cells, the pathways are derived from a DEM with a random walk and Monte Carlo simulation. Three of the methods implemented for run-out distance calculation, an empirical model and two process-based models, are compared in detail regarding their applicability for natural hazard zonation and the analysis of geomorphic activity. Several examples are presented both at a regional and a slope scale. The empirical model – the minimum shadow angle principle - provides only a first approximation of run-out length. The process-based models allow more accurate predictions. The model simulating the motion of a rock as a succession of flying and contact phases performs slightly better than a model that considers the rock to slide over the slope surface. The former also accounts for collisions with tree trunks, allowing to investigate the protection function of forest in great detail. The latter is easier to use as it requires less input data.

1 Introduction

Among other geomorphic processes, rockfall is very frequent in mountainous areas. Rockfall is defined as the movement of rock by free fall, bouncing, rolling and sliding. The term is usually restricted to small events, from single rock fragments up to events of 10 000 m^3, which are characterized by negligible interaction among the falling rocks. In contrast, large-scale mass movements of rock material are defined as rockslides or rock avalanches (e.g. ABELE 1994).

Rockfall is limited to steep slopes and starts with the detachment of rocks from bedrock slopes (primary falls) or the remobilisation of loose, temporarily accumulated rocks or debris (secondary falls, RAPP 1960). On very steep slopes (> 70°), the first mode of motion is free fall. 75 to 86% of the energy gained in this initial fall is lost in the first impact on the slope surface (BROILLI 1974). The first impact is usually followed by a sequence of bounces. With decreasing slope gradient, a bouncing rock gradually transforms its motion to rolling. Sliding occurs mostly in the initial and final stages of a rockfall. The velocity and therefore the stopping of a rock mainly depends on the mean slope gradient (DORREN 2003).

Rockfall is always a rapid phenomenon and the unpredictability of a single event potentially endangers human lives and infrastructure. A very efficient way to assess the risk posed by rockfall is to use a simulation model. A comprehensive review of rockfall models is given by DORREN (2003), who categorized these models into three

main groups: empirical models, process-based models and GIS-based models. The latter are either empirical or process-based. In general, it is necessary to distinguish slope-scale models, mostly used in rockfall engineering, from models applicable at a regional scale. In the latter case, a model must include three procedures: automatic identification of rockfall source areas, automatic determination of pathways and the calculation of run-out distance. This is why GIS-based models are favourable at a regional scale. At best, the models are integrated into a GIS environment instead of being loosely coupled to a GIS, making data transfer between the model and the GIS unnecessary. Input data preparation and output analysis are conveniently performed within a GIS.

In this paper, we give an overview about some raster-based models we implemented as SAGA module libraries in order to evaluate rockfall activity at local and regional scales. We compare the results obtained from three different models: a simple empirical model and two process-based models differing in the detail of process representation. In addition, the applicability of the models to investigate the sediment transfer (i.e. the geomorphic activity) by rockfall and for natural hazard zonation is discussed. Model application is demonstrated in the Reintal, an alpine basin south of Garmisch-Partenkirchen, Germany.

2 Methods and Model Components

This part of the paper gives a brief review of the methods we implemented as SAGA module libraries. We choose SAGA because of the following reasons: (a) the models are directly integrated in a GIS environment; (b) the easy to use application programming interface (API) and (c) the speed of calculation. Together with the methods used for determining rockfall source areas, pathways and run-out distances, the methods used for evaluating geomorphic activity and natural hazard are described.

Rockfall source areas: The location and mass of the rocks that will eventually become a rockfall are uncertain. The materials that make up a slope can vary considerably from one section of the slope to the other and the relevant material properties are usually not well known. This applies notably to rockfall modelling at a regional scale where input data is usually of limited accuracy. A common method for automatically identifying rockfall source areas is to derive a slope gradient map from a digital elevation model (DEM) and to apply a threshold to that grid (e.g. VAN DIJKE & VAN WESTEN 1990). As rockfall initiation is strongly correlated to steep slopes, this method normally yields satisfactory results. Typical slope thresholds applied range from 30° to 60° (e.g. TOPPE 1987; VAN DIJKE & VAN WESTEN 1990). Calculation of slope gradient from DEMs and its reclassification to source cells is easily done with existing SAGA modules. The results might be improved by taking further information like geological or land cover information into account (e.g. DORREN & SEIJMONSBERGEN 2003).

Pathways: The behaviour of rockfalls is influenced by slope and rock geometry as well as by slope and rock material properties. As a result of the interaction of these factors, the exact path a rockfall will take is unpredictable (PFEIFFER & BOWEN 1989). The physical process of a rockfall is very sensitive to small changes in these parameters. A very common method to determine pathways is the D8 method

described by O'CALLAGHAN & MARK (1984). This method, originally developed for the extraction of drainage networks from DEMs, calculates the fall direction as the direction of the steepest descent towards a neighbouring cell in a moving 3x3 window. It yields unsatisfactory results when applied to rockfall. Instead of generating diverging run-out zones as usually observed in the field, the method is only capable of calculating converging pathway patterns.

A better approach is to calculate pathways with multiple-flow direction algorithms (e.g. QUINN et al. 1991; TARBOTON 1997; DORREN et al. 2004). These algorithms make it possible to simulate diverging pathway patterns. As they were normally developed for hydrological applications, all lower neighbours of the central cell in the moving window are selected as pathways, regardless of the slope gradient to these cells. This may result in an overestimation of the magnitude of divergence in steep sections of the slope profile. For a simulation of mass movements like rockfall, an algorithm that takes into account the local relief to calculate the magnitude of divergence yields more realistic results. Therefore we use the mfdf method (GAMMA 2000) to calculate potential pathways. The method is implemented as a random walk in conjunction with a Monte Carlo approach and allows for calibrating the amount of modelled divergence by three parameters: (a) a slope threshold, above which no divergence is modelled (i.e. single-flow direction, D8). In case the maximum gradient is lower than the slope threshold, the gradients to all lower neighbouring cells are divided by the threshold to obtain relative slope gradients. Together with (b) a parameter that controls the magnitude of divergence, this ratio is then used as a criterion whether a neighbouring cell exhibits a sufficiently high gradient to be selected as potential pathway. The transition probabilities of all neighbouring cells that meet the criterion are calculated proportional to the sum of their relative slope gradients; (c) a persistence factor that allows to increase the probability of that neighbouring cell, which features the same direction like the centre cell was entered.

The calculated probabilities are used to select one of the neighbouring cells as pathway by random and the procedure is repeated until a stopping criterion is met (e.g. the velocity becomes zero). This results in different pathways for each model run from the same source cell. By calculating a sufficient amount of random walks from a source cell, the total process area is reproduced. A more detailed description of the method and its implementation is given by WICHMANN & BECHT (2005) and WICHMANN (2006).

Run-out distance: To calculate run-out distance, we implemented several methods, both empirical and process-based. The former result in a first approximation of run-out distance, because the mechanics of the process and the properties of the slope surface are not considered. Two common methods applied are the equivalent friction angle method (e.g. TOPPE 1987) and the minimum shadow angle principle (EVANS & HUNGR 1993). The former describes the angle given by the ratio of the vertical drop and the horizontal distance between the top of a rockfall source scar and the stopping position. The latter uses the highest point of the talus slope instead of the top of a scar to calculate the vertical drop. A third empirical method we implemented is the Fahrböschung principle (HEIM 1932), which is equivalent to the friction angle method besides that the horizontal distance is calculated as the distance travelled along the pathway.

Process-based models often result in more accurate predictions of run-out distances as they describe the motion of a rock taking some properties of the slope surface and/or the rock itself into account. The run-out length is calculated on the basis of the velocity of the falling rock. The slope surface is modelled as a continuous group of straight line segments connecting the centres of the grid cells.

A general and simple method which calculates the velocity of a mass that is considered to slide over a slope surface was developed by SCHEIDEGGER (1975). This method is used by various authors, e.g. van DIJKE & VAN WESTEN (1990). We implemented a modification of the method, including free fall before the first impact on the talus slope as suggested by SCHEIDEGGER (1975). The application of the method requires the determination of a friction coefficient which depends on surface cover characteristics, i.e. material properties and obstacles on the slope. Friction coefficient maps can be derived by assigning appropriate values to reclassified (engineering) geological and land-cover maps. More detailed information about the friction models described so far is given by WICHMANN (2006).

A second process-based model implemented simulates the motion of a rock as a succession of flying and contact phases. Again, the mass of the rock is considered to be concentrated in one point but the velocity is now calculated with standard equations for a uniformly accelerated parabolic movement through the air. The energy balance and thus the velocity before and after a collision (i.e. bounce) upon the slope surface is calculated with equations derived by DORREN & SEIJMONSBERGEN (2003). These are modified versions of the equations of PFEIFFER & BOWEN (1989), neglecting the factor compensating for the effect of the rockfall velocity on the elasticity of the collision. From each source cell, a single falling rock is simulated in each iteration of the Monte Carlo simulation. The rock cannot break or split into multiple pieces during the simulation. The effect of air resistance is not taken into account as it is assumed that the rocks are massive enough and travelling at low enough speeds that this can be ignored. Furthermore, considering air resistance would complicate the analysis and have little effect on the outcome of the simulation.

Before a simulation can begin, some initial boundary conditions must be defined. These are the radius and mass of the rock and the initial horizontal and vertical velocity components. Furthermore, it is possible to define an initial fall height (i.e. the height of the rock above the slope surface in the source cells) to account for the smoothed topography of the DEM compared to the real topography. A minimum velocity needs to be specified as stopping condition of the simulation.

The components of velocity are acted upon by gravitational acceleration until the rock's trajectory intersects the slope surface. The path the rock will take through the air is, because of the force of gravity, a parabola. At each impact, the incoming velocity of the rock is resolved into components tangential and normal to the slope (PFEIFFER & BOWEN 1989). To account for the variability of the slope to some degree, we randomly reduce the slope angle at the point of impact by values in the range 0° to 4° as suggested by DORREN & SEIJMONSBERGEN (2003).The outgoing velocity components after the bounce are determined by changing the incoming velocity components because of energy loss defined by the tangential and the normal coefficient of restitution. The calculation of the bounce results in a new trajectory which is used to calculate the next intersection with the slope surface. This is repeated as long the velocity after the impact is above the specified minimum velo-

city. If the distance travelled along the slope surface between two bounces is less than the diameter of the rock, the rock is considered to be rolling. In this case, the rock is given a new displacement over the slope surface equal to the distance of its diameter from its previous position. This method, originally proposed by PFEIFFER & BOWEN (1989), models a rolling rock as a series of short bounces, much like an irregular rock rolls on an irregular surface. Furthermore, the simulation of rolling by a succession of impacts and bounces has the advantage that it is unnecessary to introduce another parameter, i.e. the coefficient of friction (DORREN 2003).

The tangential coefficient of restitution is a measure of the resistance to movement parallel to the slope and the normal coefficient of restitution is a measure of the degree of elasticity in a collision normal to the slope (PFEIFFER & BOWEN 1989). The coefficients of restitution are often determined on the basis of the vegetation cover, surface roughness and the geological features of the slope. They are highly variable for the different types of bedrock, debris and soil. A common method to derive the coefficients is to perform a back-analysis after a rockfall has occurred (e.g. AZZONI et al. 1992). DORREN et al. (2006) present an equation to estimate the tangential coefficient of restitution from the maximum obstacle height at the slope surface and the radius of the falling rock.

The velocity of a falling rock is also affected by collisions with standing trees. These collisions result in a decrease of the kinetic energy and consequently of the velocity of the falling rock. The distribution of trees on forested cells along the pathway is determined by random from two (optional) input maps: one specifying the number of trees per hectare and one giving the average diameter of the tree trunk at breast height (DBH). As the model simulates the rocks as falling through the centre of the raster cells it is possible to determine whether and where a tree is hit. To estimate the fraction of energy loss due to the collision we use the formulae suggested by DORREN & SEIJMONSBERGEN (2003). Using this formulae, the energy loss is at maximum if a central collision between a rock and a tree trunk occurs (the maximum energy loss is limited to 99% as suggested by the authors). After the energy loss is calculated, the kinetic energy of the horizontal and the vertical velocity components is reduced accordingly and transformed back into a resultant velocity. In case the tree was hit while the rock was flying through the air, the post impact velocities are used as initialisation for the next parabola originating at the bottom of the tree. A deflection of the rock, i.e. a change of direction is not considered. This model component is very useful to investigate the protective function of forest. When applying the model at a slope scale, it is possible to output a table that is preformatted for easy production of slope profile plots (projectile trajectory, tree impacts, velocity, kinetic energy, height of the rock above the slope surface).

Geomorphic activity: The total area affected by rockfall is determined by the methods described above. The classification of this area into areas of erosion, transport and deposition is performed on the basis of the modelling results. Areas of erosion are congruent with the modelled rockfall source areas whereas areas of deposition result from the calculated stopping positions of the rocks. Areas in between are classified as areas of transport. In most instances there is an overlap of the modelled erosion and deposition areas, resulting in a forth class covering areas that feature erosion and deposition at the same time. It seems probable that these areas are congruent with source areas of secondary falls.

Hazard zonation: The described models allow the spatial prediction of rockfall hazard. Frequency and magnitude have to be evaluated by other means. The modelling of different magnitudes, i.e. fragment sizes, may require a recalibration of the model parameters, particularly of the friction coefficients. A further model component implemented allows to assess the elements at risk. In this case, a grid with potentially endangered objects is needed as model input. If an object is hit during the simulation, the object ID is coded both in the originating source cell and along the pathway above the object. This allows to use the model results to design safety measures.

A crude method to evaluate safety measures is also given: If an input grid with obstacle heights is specified, these heights are added to the DEM before simulation. In this case the path of a rockfall is influenced by the obstacles along the pathway.

3 Model Application

In this section we present the application of three different models for run-out distance calculation: (a) the minimum shadow angle principle, in the following called RockA, (b) the method of Scheidegger (1975) including free fall followed by sliding over the slope surface (RockB) and (c) the second process-based model described in section 2 under paragraph 'run-out distance' (RockC).

Study area: The Reintal valley, with the river Partnach, drains the Wetterstein mountain range that consists almost entirely of Wetterstein limestone, a very pure Triassic limestone. The valley has almost the perfect shape of a glacial trough, formed during the ice ages by glaciers descending from the Zugspitze, Germany's highest peak. Several cirques lie on both sides of the valley. The transversal profile of the valley is asymmetric, with steep rock faces on the right (N-facing) and moderately steep slopes on the left side (S-facing).

The Reintal covers the subalpine, alpine and subnival/nival zones, reaching elevations of over 2700 m a.s.l., with a relief of 1700 m. 75% of the study area have a very thin (insular occurrence) or no soil cover at all, the remaining area is covered by lithosols. Consequently, over two thirds of the basin are free of vegetation or covered with pioneer vegetation, only 9% are forested (14% krummholz). Due to karst formation and subsurface drainage in the Wettersteinkalk limestone, gravitational processes like rockfall or debris flows occur on a much larger scale than fluvial processes.

The massive Wetterstein limestone is geomorphologically very stable forming steep slopes and rockwalls. The production of rock fragments available to rockfall is equally active on all the steep cliff faces throughout the study area. The slope gradient within the source areas of rockfall varies between 40° and 90°. The accumulation areas are steep talus cones with slope gradients up to 40°.

Input data: Because of the great influence of topography on rockfall, a digital elevation model is the most relevant input dataset. We interpolated a DEM with a cell size of 5x5 m from photogrammetrically derived contour lines (20 m, © Bayerisches Landesver-messungsamt München) and additional information about (transport) channels in a two step procedure with ArcInfos Topogrid module. A first interpolation without smoothing was used to create contour lines with an equidis-

tance of 10 m. These contour lines were used to complete the original dataset. The combined dataset was finally used to interpolate a smoothed DEM.

The DEM was used to calculate a slope map (maximum slope method) from which the rockfall source areas were extracted by applying a threshold of 40°. All areas with slope gradients lower than 40° were used to define the top of the talus cones within RockA: the first time a pathway reaches this area, the calculation and supervision of the shadow angle begins.

For the application of RockB and RockC either a spatially distributed friction coefficient map or maps with tangential and normal restitution coefficients are needed. These maps were obtained by reclassifying a land cover map (mapped from orthophotos, © Bayerisches Landesvermessungsamt München) with attribute data estimated on the basis of published data (PFEIFFER & BOWEN 1989; VAN DIJKE & VAN WESTEN 1990; AZZONI et al. 1992; DORREN & SEIJMONSBERGEN 2003) and field work (see Tab.1). To obtain more realistic velocities and thus a better reproduction of run-out length, the estimated friction within the cliff faces and on bare scree slopes is relatively high compared to values reported in other studies. The steep rockwalls feature a stepped profile with intermediary flat sections on which loose material is accumulated. Small ledges are insufficiently represented in the DEM because of the input data quality and the cell size. The amount of energy loss on bare scree slopes is increased because the surface is covered by large, loosely bedded rocks.

Tab.1: Coefficient of friction (μ) and tangential and normal coefficients of restitution (r_t and r_n) used for the different land cover classes

Land cover	μ	r_t	r_n
Steep slope (40-90°)	0.90	0.50	0.45
Bare scree slope	0.90	0.45	0.32
Scree slope with thin soil cover	0.80	0.72	0.30
Meadow	0.60	0.78	0.28
Krummholz	0.90	0.50	0.28
Bushes	0.65	0.60	0.28
Forest	1.40	0.78[1]	0.28[1]

[1] These values are only used if no collisions with tree trunks occur (see text for explanation)

In RockB, the collision with tree trunks in forested areas is not modelled in detail. To account for higher energy losses in these areas, the friction coefficient is set to a higher value. To model the collision with tree trunks with RockC, two further input maps are required: a map with the number of trees per hectare and a map with the average DBH per cell. This data was roughly estimated by visual inspection of orthophotos and knowledge from field work. We assume 500 trees per hectare and an average DBH of 0.3m. Finally a map with potentially endangered objects was produced by mapping the hiking trails and Alpine huts from topographical maps and orthophotos.

Model parameters: The model parameters were chosen to simulate a high magnitude event, i.e. a worst case scenario. All three models were run with the same random walk parameters: a slope threshold of 65° (in accordance with the parameter used for free fall in RockB), a divergence parameter of 2 and a persistence factor of 1.

- In RockB, free fall is modelled as long as the gradient along the pathway is greater than 65°. The fraction of energy lost in the first impact is set to 75% in accordance with BROILLI (1974).
- In RockC, the following initial boundary conditions were used: a radius of 0.25m, a mass of 150 kg, an initial velocity in horizontal direction of 1 m/s and in vertical direction of –1 m/s. The initial fall height in all rock source cells was set to 3m.
- In RockA, the maximum run-out distance was defined by a shadow angle of 30°. In RockB and RockC, a velocity threshold is used to define the stopping criteria (0 m/s and 0.5 m/s respectively).

4 Results and Discussion

A map of the geomorphic activity resulting from the application of RockC is shown in Plate 13 (Appendix). The map shows the modelled areas of erosion, transport and deposition. Because of the extreme topographic conditions in the Reintal valley, areas of erosion are in good agreement with the steep rockwalls. The areas exhibiting both erosion and deposition correspond with the flat ledges within the rockwalls. A special case are the areas of erosion in the 'Feldernjöchl', located in the SW of the study area. Here, the ridge is covered up with loose debris (moraine) and thus mainly secondary falls are released. Areas of transport lie between the areas of erosion and deposition. Deposition is modelled in two different altitudinal belts: on scree slopes within the cirques on both sides of the valley and on screes located on the valley floor below the rockwalls. In forested areas, the run-out length is considerably shorter due to collisions with tree trunks.

As the areas of erosion are the same for all three models, we study the performance of the models by comparing the areas modelled as deposition in greater detail. The percentage of the study area modelled as deposition area by RockA amounts to 19.4%. This is a relatively small value compared to those portions resulting from RockB (48.2%) and RockC (46.1%) and a consequence of the shadow angle principle. Although the pathways from one source cell vary considerably, the shadow angle is under-run more or less at the same distances from the source. Thus the match of the deposition areas modelled by RockA and those produced by the other two models is relatively poor (32% and 34% resp. see Tab.2).

In contrast, the depositional areas of RockB and RockC overlap by 65%. The good agreement of the number of cells without deposition modelled by RockA and the other two models (92% and 93% respectively) results from the small area that is modelled as deposition area by RockA. The association between the modelled patterns of deposition, given by the ϕ-coefficient (BURT & BARBER 1996), is not very strong for all the three models ($\phi_{AB} = 0.30$; $\phi_{AC} = 0.34$; $\phi_{BC} = 0.37$), although the simulation results of RockB and RockC are quite similar.

Tab.2: Contingency tables of the three models presenting the accuracies normalized for the number of modelled cells (deposition / no deposition)

	RockB deposition	RockB no deposition	Total
RockA deposition	0.32	0.08	0.40
RockA no deposition	0.68	0.92	1.60
Total	1.00	1.00	

	RockC deposition	RockC no deposition	Total
RockA deposition	0.34	0.07	0.41
RockA no deposition	0.66	0.93	1.59
Total	1.00	1.00	

	RockB deposition	RockB no deposition	Total
RockC deposition	0.65	0.28	0.94
RockC no deposition	0.35	0.72	1.06
Total	1.00	1.00	

The largest differences appear on forested slopes: while RockC shows deposition on both forested and non-forested slopes throughout the study area, RockB shows only small areas of deposition on forested slopes. This is the result of the comparatively high friction coefficient used for forested areas in RockB and in good agreement with findings of Dorren and Seijmonsbergen (2003). They assign a model comparable to RockC the best overall performance in forested areas. A detailed slope profile with the trajectory of the falling rock and its velocity, kinetic energy and height above the slope surface is shown in Figure 1. The profile is located west of the map shown in Plate 15 (Appendix). There are several collisions with tree trunks (one is marked in Figure 1) resulting in a high loss of energy.

In general, the great vertical drop and the complex topography within the rock-walls makes the modelling of run-out length difficult. Plate 14 (Appendix) shows the modelled stopping positions on the talus scree above the location 'Vordere Blaue Gumpe', a small temporary lake dammed by a rockslide. The maximum vertical drop at this location is approximately 900 m and the chosen source cell is located about 400 m above the valley floor. A slope profile along the steepest descent is shown in Figure 2. Besides the trajectory of RockC, the maximum run-out length of each model is marked. The application of RockA results in three spatially more or less disconnected deposition areas: One located directly beneath the rockwall, one at the end of the scree slope and one far below at the end of the shown profile. The uppermost deposition area results from model runs detecting the highest point on the talus scree correctly. The obvious overestimation of the run-out length in the third case results from pathways that cross a flat ledge located in the rockwall at horizontal distance of about 75 m. As these ledges exhibit slope gradients below 40°, they are used by the model as the highest point of the talus scree. In this case, an angle of 30° is too small to force an earlier stopping of the rocks. The overestimation becomes worse the higher these ledges are located within the rockwall. For rocks triggered at the ridge of the rockwall (approx. 900 m above the valley floor) this results in a run-out length of nearly 1500 m. Some rocks come to rest earlier and build up the deposition area in the middle. The different stopping positions are the result of different pathways calculated by the path finding algorithm.

The stopping positions modelled by RockB are located approximately in the middle of the scree slope and are scattered over a wider area. The velocity profile shown in Figure 2 reveals the large amount of energy dissipated in the first impact on the scree slope (approx. at 50 m distance). After the impact, the rock gathers further speed before the velocity is continuously decreasing. The modelled maximum run-out length is in good agreement with field observations of larger boulders. Rocks detached farther upslope at the top of the rockwall accumulate at the end of the scree slope. Thus the choice of a relatively high friction coefficient for bare scree slopes yields good results overall. The stopping positions modelled by RockC are even more scattered and cover more or less the whole scree slope. The velocities reached are very similar to those achieved with RockB. Because the whole accumulation area observed in the field is covered by RockC, this model performs slightly better as RockB when used to delineate zones of different geomorphic activity.

An assessment of the elements at risk with RockB is shown in Plate 15. The map is located at the eastern end of the study area. Both the hiking trail and an Alpine hut ('Hochempor Hütte') are endangered. The model results show that the hazard does not emanate from the rockwalls located directly above but from walls farther upslope. Rocks detached in these heights gather enough energy to overcome the scree slope covered by forest. Quite similar results are produced by RockC.

5 Conclusion

As described above, the results of the three models differ considerably. RockA produces quite unsatisfactory results whereas the overall performance of RockB and RockC is quite good. We are in an initial stage of model application and thus there is some uncertainty in choosing the correct model parameters valid for different environmental settings. This is especially true for the friction coefficients used. Nevertheless, it is possible to draw some conclusions from the results obtained.The choice of a slope threshold to derive potential source areas of rockfall from a DEM is straightforward and yields satisfactory results when the DEM is of adequate resolution. Using a random walk as path finding algorithm reproduces well the natural variability of rock trajectories and provides better results than other algorithms mainly developed for hydrological applications. A fact one has to bear in mind is that the algorithm strictly follows the topography. This means that the algorithm is not capable to overcome obstacles even if the rock is far above the slope surface.

From all the three methods tested for run-out length calculation, the minimum shadow angle principle performs worst. This is, as already mentioned above, mostly attributed to the complex topography of the rockwalls. Flat ledges within the rockwalls result in a large overestimation of run-out length. On non-forested slopes both of the process based models yield results consistent with field observations. On forested slopes, RockC performs slightly better. It is likely that this may be compensated by a recalibration of the friction parameter used for forest cover in RockB. The benefit of RockB is its low demand regarding the amount of necessary input data. Very detailed simulations, even on a slope scale, can be done with RockC. But this requires more detailed information about the environmental setting which is often difficult to obtain. At a regional scale, the assumptions necessary to complete the input data set may explain why RockB and RockC produce quite similar results.

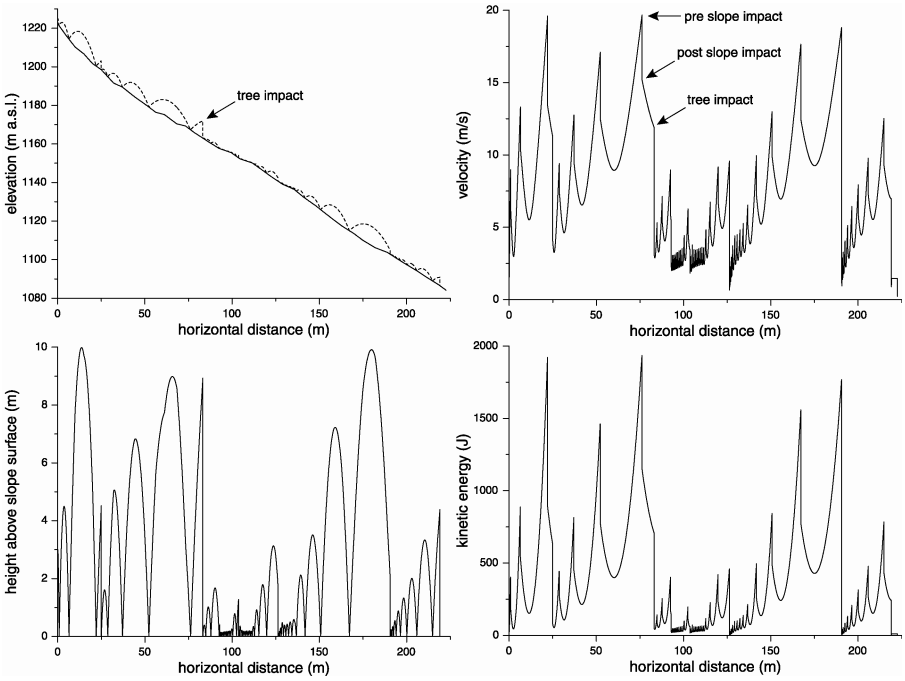

Fig.1: Profile output of RockC: (a) slope profile and projectile trajectory, (b) velocity, (c) height above the slope surface and (d) kinetic energy.

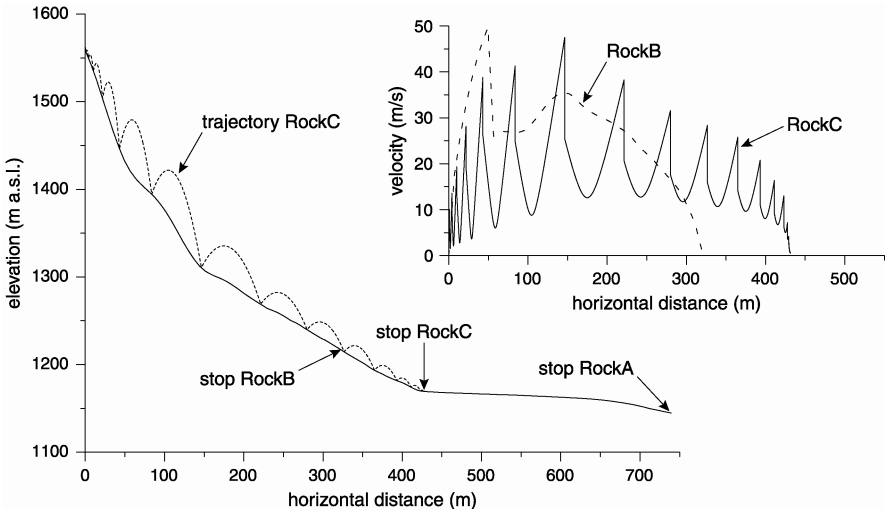

Fig.2: Profile located on the talus scree south of the temporary lake 'Vordere Blaue Gumpe'

Acknowledgements: Parts of this study are funded by the German Science Foundation (DFG, Bonn), which is gratefully acknowledged by the authors.

References

ABELE, G. (1994): Large rockslides: their causes and movement on internal sliding planes. – Mountain Research and Development 14(4): 315-320.

AZZONI, A., ROSSI, P.P., DRIGO, E., GIANI, G.P. & ZANINETTI, A. (1992): In situ observation of rockfall analysis parameters. – In: BELL, D.H. [ed.]: Proceedings of the International Symposium on Landslides, Rotterdam, Netherlands: 307-314.

BROILLI, L. (1974): Ein Felssturz im Großversuch. – Rock Mechanics, Suppl. 3: 69-78.

BURT, J.E. & BARBER, G.M. (1996): Elementary Statistics for Geographers. – Guilford Press, New York, 640 pp.

DORREN, L.K.A. & SEIJMONSBERGEN, A.C. (2003): Comparison of three GIS-based models for predicting rockfall runout zones at a regional scale. – Geomorphology 56: 49-64.

DORREN, L.K.A. (2003): A review of rockfall mechanics and modelling approaches. – Progress in Physical Geography 27(1): 69-87.

DORREN, L.K.A., BERGER, F. & PUTTERS, U.S. (2006): Real-size experiments and 3-D simulation of rockfall on forested and non-forested slopes. – Natural Hazards and Earth System Sciences 6: 145-153.

DORREN, L.K.A., MAIER, B., PUTTERS, U.S. & SEIJMONSBERGEN, A.C. (2004): Combining field and modelling techniques to assess rockfall dynamics on a protection forest hillslope in the European Alps. – Geomorphology 57: 151-167.

EVANS, S.G. & HUNGR, O. (1993): The assessment of rockfall hazard at the base of talus slopes. – Canadian Geotechnical Journal 30: 620-636.

GAMMA, P. (2000): dfwalk - Ein Murgang-Simulationsprogramm zur Gefahrenzonierung. – Geographica Bernensia G66, 144 pp.

HEIM, A. (1932): Bergsturz und Menschenleben. – Beiblatt zur Vierteljahrschrift der Naturforschenden Gesellschaft in Zürich 77, 218 pp.

O'CALLAGHAN, J. & MARK, D. (1984): The extraction of drainage networks from digital elevation data. – Computer Vision, Graphics and Image Processing 28: 323-344.

PFEIFFER, T.J. & BOWEN, T.D. (1989): Computer Simulation of Rockfalls. – Bulletin of the Association of Engineering Geologists XXVI(1): 135-146.

QUINN, P., BEVEN, K., CHEVALLIER, P. & PLANCHON, O. (1991): The prediction of hillslope flow paths for distributed hydrological modelling using digital terrain models. – Hydological Processes 5: 59-79.

RAPP, A. (1960): Recent development of mountain slopes in Kaerkevagge and surroundings, northern Scandinavia. – Geografiska Annaler A42: 65-200.

SCHEIDEGGER, A.E. (1975): Physical aspects of natural catastrophes. – Amsterdam/New York: Elsevier, 289 pp.

TARBOTON, D.G. (1997): A new method for the determination of flow directions and upslope areas in grid digital elevation models. – Water Resources Research 33(2): 309-319.

TOPPE, R. (1987): Terrain models - A tool for natural hazard mapping. – IAHS Publications 162: 629-638.

VAN DIJKE, J.J. & VAN WESTEN, C.J. (1990): Rockfall Hazard: a Geomorphologic Application of Neighbourhood Analysis with ILWIS. – ITC Journal 1990(1): 40-44.

WICHMANN, V. & BECHT, M. (2005): Modeling of Geomorphic Processes in an Alpine Catchment. – In: ATKINSON, P.M., FOODY, G.M., DARBY, S.E. & WU, F. [eds.]: GeoDynamics: 151-167.

WICHMANN, V. (2006): Modellierung geomorphologischer Prozesse in einem alpinen Einzugsgebiet – Abgrenzung und Klassifizierung der Wirkungsräume von Sturzprozessen und Muren mit einem GIS. – Eichstätter Geographische Arbeiten 15, München/Wien: Profil Verlag, 231 pp.